

## High-pressure infrared spectroscopy on quasi-one-dimensional metals

Christine A. Kuntscher, Simone Frank, I. Loa, K. Syassen, Frank Lichtenberg, T. Yamauchi, Y. Ueda

### Angaben zur Veröffentlichung / Publication details:

Kuntscher, Christine A., Simone Frank, I. Loa, K. Syassen, Frank Lichtenberg, T. Yamauchi, and Y. Ueda. 2006. "High-pressure infrared spectroscopy on quasi-one-dimensional metals." *Infrared Physics & Technology* 49 (1-2): 88–91.  
<https://doi.org/10.1016/j.infrared.2006.01.022>.

### Nutzungsbedingungen / Terms of use:

licgercopyright

Dieses Dokument wird unter folgenden Bedingungen zur Verfügung gestellt: / This document is made available under these conditions:

#### Deutsches Urheberrecht

Weitere Informationen finden Sie unter: / For more information see:

<https://www.uni-augsburg.de/de/organisation/bibliothek/publizieren-zitieren-archivieren/publiz/>



# High-pressure infrared spectroscopy on quasi-one-dimensional metals

C.A. Kuntscher <sup>a,\*</sup>, S. Frank <sup>a</sup>, I. Loa <sup>b</sup>, K. Syassen <sup>b</sup>, F. Lichtenberg <sup>c</sup>,  
T. Yamauchi <sup>d</sup>, Y. Ueda <sup>d</sup>

<sup>a</sup> *Physikalisches Institut, Universität Stuttgart, Pfaffenwaldring 57, D-70550 Stuttgart, Germany*

<sup>b</sup> *Max-Planck-Institut für Festkörperforschung, Heisenbergstr. 1, D-70569 Stuttgart, Germany*

<sup>c</sup> *Experimentalphysik VI, Institut für Physik, EKM, Universität Augsburg, Universitätsstr. 1, D-86135 Augsburg, Germany*

<sup>d</sup> *Institute for Solid State Physics, University of Tokyo, Tokyo, Japan*

## 1. Introduction

Quasi-one-dimensional (quasi-1D) metals are characterized by highly anisotropic electronic properties related to their anisotropic crystal structure, where the structural units are arranged in chains or stacks. A large overlap of the electronic orbitals along the chains (i.e., the large charge transfer integral  $t_{\parallel}$ ) enables a coherent motion of the charge carriers along this direction, whereas along the perpendicular directions only an incoherent hopping motion is possible (i.e.,  $t_{\perp} \ll t_{\parallel}$ ). The anisotropic electronic properties can be probed directly by polarization-dependent optical spectroscopy: along the conducting crystal direction, the reflectivity is high at low frequencies and often exhibits a sharp plasma edge, whereas for the perpendicular directions the overall reflectivity is low. Furthermore, quasi-1D metals often exhibit instabilities due to electronic correlations, like charge ordering or spin-density-wave for-

mation, or due to electron–phonon coupling, like a Peierls transition accompanied by charge-density-wave formation. Such instabilities generally cause a metal-to-insulator transition. Strong electron–phonon coupling can also lead to a self-trapping of the charge carriers [1]: the displacement of atoms around the charge carrier from their carrier-free equilibrium position causes a potential well in which the carrier is trapped. Thus, a polaron is formed, i.e., a quasi-particle composed of the self-trapped carrier together with the pattern of atomic displacements, which produces the self-trapping. Characteristic signatures of polarons can be found in the optical response in the form of a pronounced absorption band located in the mid-infrared (MIR) frequency range [2].

The application of external pressure to a quasi-1D system will typically enhance the interaction between the chains or stacks that characterize its crystal structure (increase of  $t_{\perp}$ ). This may induce a dimensional crossover that can be detected in the polarization-dependent optical response. Also, the electron–phonon coupling should be affected by pressure, thus allowing a test of the polaronic picture.

---

\* Corresponding author. Tel.: +49 711 685 4942; fax: +49 711 685 4886.  
E-mail address: kuntscher@physik.uni-stuttgart.de (C.A. Kuntscher).

For the two quasi-1D metals  $\beta\text{-Na}_{0.33}\text{V}_2\text{O}_5$  and  $\text{LaTiO}_{3.41}$  along the conducting axis a pronounced MIR absorption band was observed, which was interpreted in terms of polaronic excitations [3,4]. We carried out polarization-dependent MIR reflectance measurements on these two compounds as a function of pressure to test the proposed polaronic picture. Furthermore, the pressure-induced dimensional crossover could be probed.

The crystal structure of  $\beta\text{-Na}_{0.33}\text{V}_2\text{O}_5$  consists of three kinds of chains along the conducting  $b$  axis, built by three crystallographically inequivalent V sites: zigzag double chains composed of edge-sharing (V1) $\text{O}_6$  octahedra, two-leg ladders composed of corner-sharing (V2) $\text{O}_6$  octahedra, and zig-zag double chains of edge-sharing (V3) $\text{O}_5$  polyhedra, oriented along the  $b$  axis [5]. At ambient pressure  $\beta\text{-Na}_{0.33}\text{V}_2\text{O}_5$  undergoes three phase transitions as a function of temperature [6,7]: ordering of the sodium ions at 240 K, a metal–insulator transition at around 135 K caused by charge ordering on the V sites [8] due to electronic correlations, and an antiferromagnetic transition at 22 K. Recently, the pressure–temperature phase diagram was investigated by dc resistivity and ac susceptibility measurements for pressures  $P$  up to 9 GPa [9]. A superconducting phase in proximity to the charge ordered phase was found for temperatures below 10 K and pressures higher than 7 GPa. At  $P \approx 9$  GPa superconductivity is suppressed again.

$\text{LaTiO}_{3.41}$  consists of perovskite-like slabs of vertex sharing  $\text{TiO}_6$  octahedra separated by additional oxygen layers [10,4]. The slabs are five octahedra wide, and neighboring slabs are shifted along the  $a$  axis by half an octahedron. The metallic behavior of the material along the  $a$  axis might be related to the chains of octahedra, connected via their apical oxygen atoms. The application of external pressure up to  $P = 18$  GPa leads to continuous changes of the crystal structure [11]: The axis compressibilities are anisotropic with a ratio of approximately 1:2:3 for the  $a$ ,  $b$ , and  $c$  axes. The large compressibility along  $c$  results from the highly compressible oxygen-rich layers separating the  $\text{LaTiO}_3$ -type slabs. The difference in compressibilities causes an increase of the monoclinic angle from  $97.17^\circ$  to  $97.43^\circ$  with increasing pressure. From the pressure dependence of the lattice parameters the octahedral tilt angle was estimated to double at 18 GPa compared to ambient conditions.

## 2. Experimental technique

Single crystals of  $\beta\text{-Na}_{0.33}\text{V}_2\text{O}_5$  were grown as reported in Ref. [6]. The quality of the crystals used for the high-pressure experiments was checked by dc resistivity measurements showing a sharp metal–insulator transition around 135 K. The investigated  $\text{LaTiO}_{3.41}$  crystals were grown by a floating zone melting process, and their oxygen content was determined by thermogravimetric analysis [10].

Pressure-dependent reflectance measurements on  $\beta\text{-Na}_{0.33}\text{V}_2\text{O}_5$  and  $\text{LaTiO}_{3.41}$  crystals for the polarization

$\mathbf{E}$  of the incident radiation along and perpendicular to the conducting axes were performed in the MIR frequency range ( $600\text{--}8000\text{ cm}^{-1}$ ) at room temperature, using a Bruker IFS 66v/S Fourier transform infrared spectrometer. The measurements were carried out partly in the lab at the University of Stuttgart and partly at the infrared beam-line of the synchrotron radiation source ANKA near Karlsruhe. A diamond anvil cell equipped with type IIA diamonds suitable for infrared measurements was used to generate pressures up to 20 GPa. Finely ground KCl was used as a quasi-hydrostatic pressure transmitting medium. To focus the beam onto the small sample in the pressure cell, an infrared microscope coupled to the spectrometer with a  $15\times$  magnification objective was used. An aperture of 0.6 mm diameter was chosen, which yields an IR spot of 40  $\mu\text{m}$  diameter at the sample. For the pressure experiment, the sample was polished to a thickness of  $\approx 40\text{ }\mu\text{m}$ . Before loading the pressure cell, the reflectivity of the free-standing polished samples was checked and found to be in good agreement with earlier results [3,4]. For the pressure experiment, a small piece (about  $80 \times 80\text{ }\mu\text{m}$ ) was cut and placed in the hole (150  $\mu\text{m}$  in diameter) of a steel gasket. For the pressure determination by the ruby luminescence method [12], a small ruby chip was added. Reflection spectra were measured at the interface between sample and diamond. Spectra taken at the inner diamond–air interface of the empty cell served as the reference for normalization of the sample spectra. The absolute reflectivity at the sample–diamond interface, denoted as  $R_{s-d}$ , was calculated according to:  $R_{s-d}(\omega) = R_{\text{dia}} \times I_s(\omega)/I_d(\omega)$ , where  $I_s(\omega)$  denotes the intensity spectrum reflected from the sample–diamond interface and  $I_d(\omega)$  the reference spectrum.  $R_{\text{dia}}$  was determined from the refractive index of diamond  $n_{\text{dia}}$  to 0.167 and assumed to be independent of pressure; this is justified since  $n_{\text{dia}}$  is known to change only very little with pressure ( $-0.00075/\text{GPa}$ ) [13,14]. Variations in source intensity were taken into account by applying additional normalization procedures.

To obtain the corresponding optical conductivity, the reflectivity spectra were fitted with the Drude-Lorentz model combined with the normal-incidence Fresnel equation, taking into account the known refractive index of diamond. Furthermore, an increase of the background dielectric constant (by 15% at maximum) according to the Clausius–Mossotti relation [15] was assumed to account for the pressure-induced reduction of the unit cell volume [16,11].

## 3. Results

Pressure-dependent reflectivity spectra  $R_{s-d}$  of  $\beta\text{-Na}_{0.33}\text{V}_2\text{O}_5$  are presented in Fig. 1 for the polarizations  $\mathbf{E} \parallel b$  and  $\mathbf{E} \perp b$ . (The region around  $2000\text{ cm}^{-1}$  is cut out from the experimental spectra since the diamond multi-phonon absorption causes artifacts in this range; the features at  $\omega \approx 2500$  and  $3700\text{ cm}^{-1}$  are artifacts that originate from multiphonon absorptions of diamond that are not fully

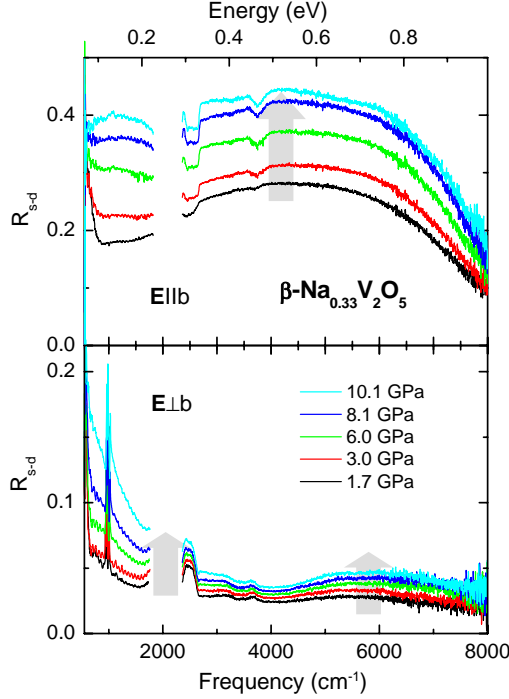


Fig. 1. Room temperature reflectivity spectra  $R_{s-d}$  of  $\beta\text{-Na}_{0.33}\text{V}_2\text{O}_5$  as a function of pressure for the polarization  $\mathbf{E}$  parallel and perpendicular to the conducting  $b$  axis. The arrows indicate the changes with increasing pressure.

corrected by the normalization procedure.) Corresponding pressure-dependent optical conductivity spectra of  $\beta\text{-Na}_{0.33}\text{V}_2\text{O}_5$  for the polarization along the conducting axis, i.e.,  $\mathbf{E}||b$ , are presented in Fig. 2; they show a pronounced MIR absorption band, consistent with earlier results [3]. With increasing pressure the overall reflectivity along both directions rises monotonically (see Fig. 1), indicating a growing spectral weight in the infrared response. Corre-

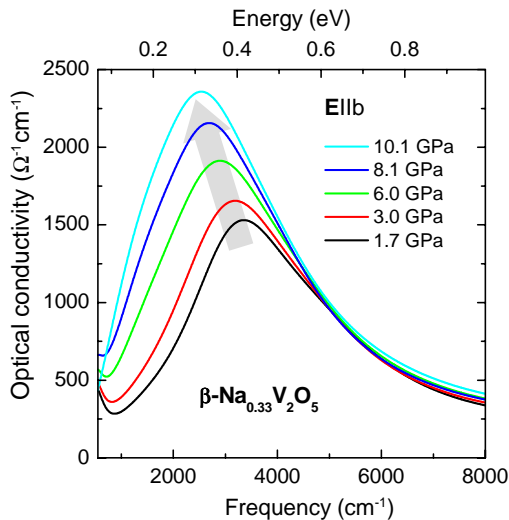


Fig. 2. Room temperature optical conductivity spectra of  $\beta\text{-Na}_{0.33}\text{V}_2\text{O}_5$  as a function of pressure for the polarization  $\mathbf{E}$  parallel to the conducting  $b$  axis. The arrow indicates the changes with increasing pressure.

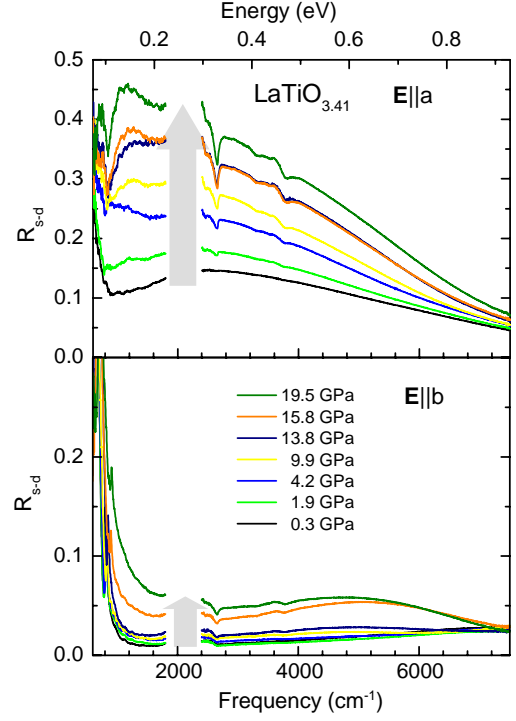


Fig. 3. Room temperature reflectivity spectra  $R_{s-d}$  of  $\text{LaTiO}_{3.41}$  as a function of pressure for the polarization  $\mathbf{E}$  along the conducting  $a$  axis and along the  $b$  axis. The arrows indicate the changes with increasing pressure.

spondingly, the oscillator strength of the pronounced  $\mathbf{E}||b$  MIR band in the optical conductivity increases (Fig. 2); its maximum shifts to lower frequencies. The most notable effect on the  $\mathbf{E}\perp b$ -spectra is a strong increase of  $R_{s-d}$  in the low-frequency ( $\omega < 2000 \text{ cm}^{-1}$ ) range. At around 12 GPa we find marked changes, as reported in Ref. [17].

The results of the pressure-dependent reflectivity  $R_{s-d}$  and optical conductivity of  $\text{LaTiO}_{3.41}$  are shown in Figs. 3 and 4, respectively. For the polarization along the chains,  $\mathbf{E}||a$ , the overall reflectivity increases monotonically with increasing pressure. In contrast, for  $\mathbf{E}||b$  the reflectivity

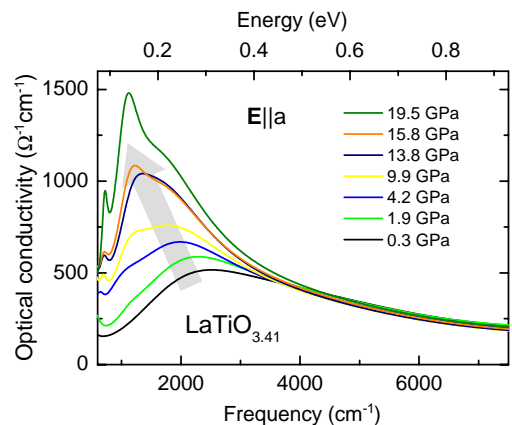


Fig. 4. Room temperature optical conductivity spectra of  $\text{LaTiO}_{3.41}$  as a function of pressure for the polarization  $\mathbf{E}$  along the conducting  $a$  axis. The arrow indicates the changes with increasing pressure.

remains basically unchanged up to a pressure of  $\approx 14$  GPa; only above this pressure the reflectivity increases significantly, in particular in the low-frequency range. Similar to the results of  $\beta\text{-Na}_{0.33}\text{V}_2\text{O}_5$ , the MIR optical conductivity of  $\text{LaTiO}_{3.41}$  for  $E \parallel a$  exhibits a pronounced absorption band (see Fig. 4). Qualitatively, it shows the same pressure dependence as in  $\beta\text{-Na}_{0.33}\text{V}_2\text{O}_5$ , namely an intensity increase and a shift to smaller frequencies with increasing pressure.

#### 4. Discussion

For both studied quasi-1D compounds  $\beta\text{-Na}_{0.33}\text{V}_2\text{O}_5$  and  $\text{LaTiO}_{3.41}$  the pressure-induced increase of the low-frequency reflectivity for the polarization perpendicular to the conducting direction suggests the onset of a pressure-induced dimensional crossover from 1D to 2D (or 3D): for  $\beta\text{-Na}_{0.33}\text{V}_2\text{O}_5$  the dimensional crossover evolves continuously starting from the lowest applied pressure. For  $\text{LaTiO}_{3.41}$  its signatures are observed only above 14 GPa. The crossover is expected to be more clearly visible in the far-infrared frequency range, where one could monitor the possible evolution of a Drude component perpendicular to the conducting axis; this is currently being investigated.

The pressure dependence of the MIR band along the chains is of particular interest, since it was claimed to be of polaronic origin [3,4]. Within small-polaron theory the frequency of the absorption band is a measure of the polaron binding energy [2], and thus of the electron–phonon coupling. In general, the electron–phonon coupling tends to decrease under pressure as a result of the combined band broadening and stiffening of the crystal lattice. So, one expects a decrease of the polaron binding energy under pressure to be a common trend. The observed redshift of the MIR band with increasing pressure thus appears to be consistent with its claimed polaronic origin. However, alternative explanations of the MIR band, for example in terms of charge transfer transitions or orbital excitations, cannot be ruled out based on our data.

#### 5. Summary

In summary, the polarization-dependent MIR optical responses of the quasi-1D metals  $\beta\text{-Na}_{0.33}\text{V}_2\text{O}_5$  and  $\text{LaTiO}_{3.41}$  were studied at room temperature as a function of pressure. Based on the low-frequency reflectivity we could monitor a pressure-induced dimensional crossover of the electronic properties. It evolves continuously in  $\beta\text{-Na}_{0.33}\text{V}_2\text{O}_5$  starting from the lowest applied pressure; for

$\text{LaTiO}_{3.41}$  indications for the crossover are found only above 14 GPa, possibly related to a structural phase transition, the onset of which was observed at 18 GPa under nearly hydrostatic conditions [11]. The pressure dependence of the pronounced MIR band observed for both compounds along the conducting axis is consistent with an explanation in terms of polaronic excitations. Alternative explanations, like charge transfer transitions or orbital excitations, however, cannot be ruled out.

#### Acknowledgements

We acknowledge the ANKA Angströmquelle Karlsruhe for the provision of beamtime and we would like to thank D. Moss, Y.-L. Mathis, and B. Gasharova for assistance using beamline ANKA-IR. Financial support by the DFG (Emmy Noether-program) is acknowledged.

#### References

- [1] L.D. Landau, Phys. Z. Sowjetunion 3 (1933) 644.
- [2] D. Emin, Phys. Rev. B 48 (1993) 13691.
- [3] C. Presura, M. Popinciuc, P.H.M. van Loosdrecht, D. van der Marel, M. Mostovoy, T. Yamauchi, Y. Ueda, Phys. Rev. Lett. 90 (2003) 026402.
- [4] C.A. Kuntscher, D. van der Marel, M. Dressel, F. Lichtenberg, J. Mannhart, Phys. Rev. B 67 (2003) 035105.
- [5] A.D. Wadsley, Acta Cryst. 8 (1955) 695.
- [6] H. Yamada, Y. Ueda, J. Phys. Soc. Jpn. 68 (1999) 2735.
- [7] Y. Ueda, H. Yamada, M. Isobe, T. Yamauchi, J. Alloys Comp. 317–318 (2001) 109;  
A.N. Vasil'ev, V.I. Marchenko, A.I. Smirnov, S.S. Sosin, H. Yamada, Y. Ueda, Phys. Rev. B 64 (2001) 174403;  
J.-I. Yamaura, M. Isobe, H. Yamada, T. Yamauchi, Y. Ueda, J. Phys. Chem. Solids 63 (2002) 957.
- [8] M. Heinrich, H.-A. Krug von Nidda, R.M. Eremina, A. Loidl, Ch. Helbig, G. Obermeier, S. Horn, Phys. Rev. Lett. 93 (2004) 116402.
- [9] T. Yamauchi, Y. Ueda, N. Môri, Phys. Rev. Lett. 89 (2002) 057002.
- [10] F. Lichtenberg, A. Herrnberger, K. Wiedenmann, J. Mannhart, Prog. Solid State Chem. 29 (2001) 1.
- [11] I. Loa, K. Syassen, X. Wang, F. Lichtenberg, M. Hanfland, C.A. Kuntscher, Phys. Rev. B 69 (2004) 224105.
- [12] H.K. Mao, J. Xu, P.M. Bell, J. Geophys. Res. (Atmos.) 91 (1986) 4673.
- [13] M.I. Erements, Y.A. Timofeev, Rev. Sci. Instrum. 63 (1992) 3123.
- [14] A.L. Ruoff, K. Ghandehari, in: S.C. Schmidt, J.W. Shaner, G.A. Samara, M. Ross (Eds.), High pressure science and technology, American Institute of Physics Conference Proceedings, vol. 309, Woodbury, NY, 1994, pp. 1523–1525.
- [15] N.W. Ashcroft, N.D. Mermin, Solid State Physics, Harcourt Brace College Publishers, Fort Worth, 1976.
- [16] J.-I. Yamaura et al., unpublished.
- [17] C.A. Kuntscher, S. Frank, I. Loa, K. Syassen, T. Yamauchi, Y. Ueda, Phys. Rev. B 71 (2005) 220502(R).